Celest Mech Dyn Astr (2013) 116:21–34
DOI 10.1007/s10569-013-9476-9

ORIGINAL ARTICLE

Robust resolution of Kepler's equation in all eccentricity regimes

Davide Farnocchia · Davide Bracali Cioci · Andrea Milani

Received: 24 July 2012 / Revised: 21 January 2013 / Accepted: 23 January 2013 /
Published online: 13 February 2013

Abstract In this paper we discuss the resolution of Kepler's equation in all eccentricity regimes. To avoid rounding off problems we find a suitable starting point for Newton's method in the hyperbolic case. Then, we analytically prove that Kepler's equation undergoes a smooth transition around parabolic orbits. This regularity allows us to fix known numerical issues in the near parabolic region and results in a non-singular iterative technique to solve Kepler's equation for any kind of orbit. We measure the performance and the robustness of this technique by comprehensive numerical tests.

Keywords Two-body problem · Kepler's equation · Newton's method · Starting points · Universal variables · Near parabolic motion

1 Introduction

The two-body problem is described by the following Initial Value Problem:

$$\frac{d^2\mathbf{r}}{dt^2} = -\frac{\mu}{r^3}\mathbf{r}, \quad r = ||\mathbf{r}||, \quad \mathbf{r}(0) = \mathbf{r}_0 \in \mathbb{R}^3, \quad \frac{d\mathbf{r}}{dt}(0) = \mathbf{v}_0 \in \mathbb{R}^3 \,. \tag{1}$$

Apart from the case in which $\mathbf{r}_0$ and $\mathbf{v}_0$ are parallel, the solution $\mathbf{r}(t)$ moves along a conic defined by the following quantities:

- pericenter distance q and eccentricity e, describing the geometry of the conic;
- inclination I, longitude of node Ω, and argument of pericenter ω, describing the position of the conic in the three dimensional space;
- true anomaly f, describing the position along the conic.

D. Farnocchia (✉) · D. Bracali Cioci
SpaceDyS s.r.l., Via Mario Giuntini 63, 56023 Cascina, PI, Italy
e-mail: farnocchia@spacedys.com

A. Milani
Department of Mathematics, University of Pisa, Largo Bruno Pontecorvo 5, 56127 Pisa, Italy

The relationship between true anomaly and time is given by

$$\int_0^f \frac{1}{(1+e\cos\nu)^2}d\nu = \sqrt{\frac{\mu}{q^3(1+e)^3}}(t-t_P) \tag{2}$$

where t_P is the time of pericenter passage.

Equation (2) can be expressed in convenient variables according to the value of the eccentricity, as described in the next three sections. Here we recall the basics needed for this paper, for a more comprehensive discussion see Colwell (1993).

1.1 Elliptic case $e < 1$

By introducing the eccentric anomaly E, which is related to f by

$$\begin{cases} \cos E = \dfrac{e+\cos f}{1+e\cos f} \\ \sin E = \dfrac{\sin f\sqrt{1-e^2}}{1+e\cos f} \end{cases}, \quad \begin{cases} \cos f = \dfrac{\cos E - e}{1-e\cos E} \\ \sin f = \dfrac{\sin E\sqrt{1-e^2}}{1-e\cos E} \end{cases}, \tag{3}$$

Eq. (2) becomes

$$\chi_E(e,E) = E - e\sin E = M_E, \quad M_E = \sqrt{\frac{\mu(1-e)^3}{q^3}}(t-t_P) \in [0, 2\pi[\,. \tag{4}$$

Equation (4) has one and only one solution and can be numerically solved by applying Newton's method:

$$E_{k+1} = E_k - \frac{E_k - e\sin E_k - M_E}{1-e\cos E_k}\,. \tag{5}$$

A starting point assuring convergence is π. More refined starting points can be found by using a cubic approximation of Eq. (4), e.g., Mikkola (1987) or Markley (1995). Odell and Gooding (1986), Davis et al. (2010), and Calvo et al. (2013) discuss other possible choices for the starting point.

Other resolution methods can be used: Conway (1986) proposes an order 3 algorithm from Laguerre; Fukushima (1996) and Feinstein and McLaughlin (2006) use a combination of the bisection and Newton's method; Palacios (2002) employs the accelerated Newton's method; Mortari and Clocchiatti (2007) present a non-iterative approach to solve Kepler's Equation, based on non-rational cubic and rational quadratic Bézier curves.

1.2 Parabolic case $e = 1$

In the parabolic case we have Barker's equation:

$$\chi_P(D) = D + D^3/3 = M_P, \quad M_P = \sqrt{\frac{\mu}{2q^3}}(t-t_P), \quad D = \tan\frac{f}{2}\,. \tag{6}$$

This equation can be analytically solved and the solution is (Battin 1987, Chap. 4):

$$D = \frac{2AB}{1+A+A^2}, \quad A = (B+\sqrt{1+B^2})^{2/3}, \quad B = \frac{3M_P}{2}\,.$$

1.3 Hyperbolic case $e > 1$

In the hyperbolic case the relationship is the following:

$$\chi_H(e, F) = e \sinh F - F = M_H, \;\; M_H = \sqrt{\frac{\mu(e-1)^3}{q^3}}(t - t_P) \tag{7}$$

$$\tanh \frac{F}{2} = \sqrt{\frac{e-1}{e+1}} \tan \frac{f}{2} \, . \tag{8}$$

Also this equation can be solved by applying Newton's method:

$$F_{k+1} = F_k - \frac{e \sinh F_k - F_k - M_H}{e \cosh F_k - 1}.$$

The choice of the starting point for the hyperbolic case is discussed in Sect. 2.

1.4 Numerical problems

Since the inverse of $E - e \sin E$ is singular at $(e, E) = (1, 0)$, the numerical solution of Kepler's equation is not a well conditioned problem for values of (e, M) in a neighborhood of $(1, 0)$ (Danby and Burkardt 1983).

In the elliptic case there are problems when $1 - e \cos E < \delta$, where $\delta > 0$ is a small parameter. Thus, we have that

$$1 - e < 1 - e \cos E < \delta \Rightarrow e > 1 - \delta \, ,$$
$$1 - \cos E < 1 - e \cos E < \delta \Rightarrow \cos E > 1 - \delta \, .$$

Under these assumptions also the pericenter time is a singular function of f. In fact, we have that

$$t_P = t - \sqrt{\frac{q^3}{\mu(1-e)^3}}(E - e \sin E)$$

is an indeterminate form again.

The same situation arises in the hyperbolic case (Burkardt and Danby 1983) when $e \cosh F - 1 < \delta$, thus

$$e - 1 < e \cosh F - 1 < \delta \Rightarrow e < 1 + \delta \, ,$$
$$\cosh F - 1 < e \cosh F - 1 < \delta \Rightarrow \cosh F < 1 + \delta \, .$$

As $\delta \simeq 0$ the asymptotic behavior is the following:

$$e \lesssim 1 - \delta \, , \quad E \lesssim \sqrt{2\delta} \, , \quad F \lesssim \sqrt{2\delta} \, .$$

For eccentricity-true anomaly variables $(e, f) \in \mathbb{R}^+ \times \mathbb{T}^1$, by excluding the physically unallowed regions where $1 + e \cos f \leq 0$, and for a small positive $\delta > 0$, we split the set $\Omega = \{(e, f) \in \mathbb{R}^+ \times \mathbb{T}^1; \, 1 + e \cos f > 0\}$ into three sets:

- Strong Elliptic set, i.e., the subset of Ω where $1 + e \cos E(f) \geq \delta$ with $E = E(f)$ defined by (3). Here Eq. (4) can be solved without numerical singularities.
- Strong Hyperbolic set, i.e., the subset of Ω where $e \cosh F(f) - 1 \geq \delta$ with $F = F(f)$ defined by (8). Here Eq. (7) can be solved without numerical singularities.
- Near Parabolic set, i.e, the complementary of the Strong Elliptic and Strong Hyperbolic sets, where either $e = 1$, or $0 < e < 1$ and $1 - e \cos E < \delta$, or $e > 1$ and $e \cosh F - 1 < \delta$.

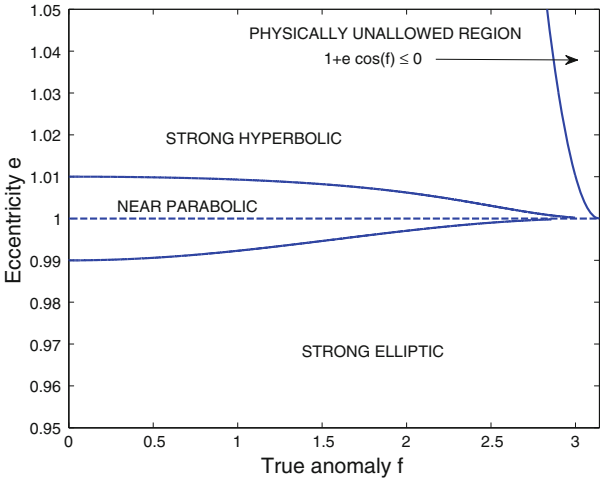

Fig. 1 Splitting of the (f, e) plane for $\delta = 10^{-2}$. The region where $1 + e \cos f \leq 0$ is not physically allowed. The region with $f > \pi$ and $e < 1$ is obtained by symmetry around $f = \pi$

Figure 1 shows the three regions for $\delta = 0.01$, $e \in [0.95, 1.05]$, and $f \in [0, \pi]$.

2 Starting point in the hyperbolic case

The choice of a starting point to solve Eq. (7) can be critical. As a matter of fact, sinh and cosh are exponential functions and therefore they can generate overflow when the argument is too large. In the simulations performed in Milani et al. (2008) we found cases in which we were not able to solve Eq. (7) because of the mentioned rounding off issues. Though the probability of this happening is rather small ($\sim 10^{-6}$), it would be very unpleasant to discover a hyperbolic comet and discard such discovery because of a failure in solving the corresponding Kepler's equation.

The following proposition gives a sensible starting point.

Proposition 1 *Let $M_H \geq 0$, then the solution F^* of* Eq. (7) *is such that:*

$$0 \leq F^* \leq F_i = \min\{\operatorname{arcsinh}[M_H/(e-1)], \log C\}$$

where $C = \exp(1)(e + 2M_H)/(e \exp(1) - 2)$. Furthermore F_i belongs to the convergence domain of Newton's method.

Proof We proceed in five steps:

- $\chi'_H(e, F) = e \cosh F - 1 > 0$, $\chi_H(e, 0) = 0$ thus $F^* \geq 0$;
- $\chi''_H(e, F) = e \sinh F > 0$ for $F > 0$, thus χ_H is convex and any point larger than F^* belongs to the convergence domain of Newton's method;
- for $F \geq 0$ we have that $M_H = \chi_H(e, F) \geq (e - 1) \sinh F$, thus $F^* \leq \operatorname{arcsinh}[M_H/(e-1)]$;
- for $F \geq 0$ we have that $F \leq \exp(F - 1)$ and $\exp(-F) \leq 1$, thus $M_H \geq e \exp(F)/2 - \exp(F - 1) - e/2$ from which we obtain $F^* \leq \log C$.

□

The starting guess F_i assures convergence and also avoids computations of too large numbers. In fact, the evaluations to be done are bounded by

$$\chi_H(e, F_i) = \min\left\{\frac{e}{2}\left(C - \frac{1}{C}\right) - \log(C), \frac{M_H}{e-1} - \operatorname{arcsinh}\left(\frac{M_H}{e-1}\right)\right\}.$$

This number can generate overflow only if M_H has the same problem, but we assume that the inputs are well defined.

If $M_H < 0$ we can use as starting point $-F_i$, here M_H is replaced by $-M_H$.

3 Regularity around $e = 1$

We introduce the variable

$$x = \frac{e-1}{1+e}D^2, \quad D = \tan\frac{f}{2}.$$

In the near parabolic region, as defined in Sect. 1.4, we have that $x \simeq \delta/2$ for δ small enough.

Theorem 1 *Let* $|x| < 1$ *and define*

$$\chi_{NP}(e, D) = \frac{\sqrt{2}}{\sqrt{1+e}}D + \frac{\sqrt{2}}{\sqrt{(1+e)^3}}D^3\, S(e, x),\ S(e, x) = \sum_{k=0}^{\infty}\left(e - \frac{1}{2k+3}\right)x^k.$$

We have that

$$\begin{cases} \dfrac{E - e\sin E}{\sqrt{2(1-e)^3}} = \chi_{NP}(e, D) & \text{for } e < 1, \\ D + \dfrac{D^3}{3} = \chi_{NP}(e, D) & \text{for } e = 1, \\ \dfrac{e\sinh F - F}{\sqrt{2(e-1)^3}} = \chi_{NP}(e, D) & \text{for } e > 1. \end{cases}$$

Proof We start from the elliptic case. The condition $|x| < 1$ assures that $f \neq \pi$. Thus, $\tan E/2 = \sqrt{-x}$ and the following Taylor's expansions hold:

$$E = 2\sum_{k=0}^{\infty}\frac{(-1)^k}{2k+1}(\sqrt{-x})^{2k+1},\ \sin E = 2\sum_{k=0}^{\infty}(-1)^k(\sqrt{-x})^{2k+1}.$$

Therefore, we have that

$$\begin{aligned}\chi_E(e, E) &= 2\sum_{k=0}^{\infty}(-1)^k\left(\frac{1}{2k+1} - e\right)(\sqrt{-x})^{2k+1} \\ &= 2\sqrt{\frac{(1-e)^3}{1+e}}\,D + 2\sqrt{\frac{(1-e)^3}{(1+e)^3}}\,D^3 S(e, x)\end{aligned}$$

and dividing by $\sqrt{2}(\sqrt{1-e})^3$ we are done.

In the parabolic case there is nothing to prove, while in the hyperbolic one $\tanh F/2 = \sqrt{x}$ and

$$F = 2\sum_{k=0}^{\infty}\frac{1}{2k+1}(\sqrt{x})^{2k+1}, \quad \sinh F = 2\sum_{k=0}^{\infty}(\sqrt{x})^{2k+1}.$$

Thus, we have that

$$\chi_H(e, F) = 2\sum_{k=0}^{\infty}\left(e - \frac{1}{2k+1}\right)(\sqrt{x})^{2k+1}$$
$$= 2\sqrt{\frac{(e-1)^3}{e+1}}\,D + 2\sqrt{\frac{(e-1)^3}{(e+1)^3}}\,D^3\,S(e, x)$$

and dividing by $\sqrt{2}(\sqrt{e-1})^3$ we are done. □

Corollary 1 *The function*

$$t_P = \begin{cases} t - \sqrt{\dfrac{q^3}{\mu}}\dfrac{E - e\sin E}{\sqrt{(1-e)^3}} & \text{for } 0 < e < 1 \\ t - \sqrt{\dfrac{2q^3}{\mu}}\left(D + \dfrac{D^3}{3}\right) & \text{for } e = 1 \\ t - \sqrt{\dfrac{q^3}{\mu}}\dfrac{e\sinh F - F}{\sqrt{(e-1)^3}} & \text{for } e > 1 \end{cases}$$

is a C^∞ function of (q, e, f) for $q > 0$, $e > 0$, and f such that $1 + e\cos f > 0$.

Proof The only thing to prove is that t_P is C^∞ for $e = 1$. Let $e \in U =]1-\varepsilon, 1+\varepsilon[$, where ε is a small parameter. Since $f \neq \pi$ and is fixed, $|x| < 1$ for ε small enough. By Theorem 1, we have that for all $e \in U$

$$t_P = t - \sqrt{\frac{2q^3}{\mu}}\chi_{NP}(e, D)\,.$$

Since $\chi_{NP} \in C^\infty$ we are done. □

Corollary 2 *Let $G(q, e, f, t - t_P)$ be*

$$G(q), e, f, t - t_P) = \begin{cases} E(e, f) - e\sin E(e, f) - \sqrt{\dfrac{\mu}{q^3}}(t - t_P)(\sqrt{1-e})^3 & \text{for } 0 < e < 1; \\ D(f) + \dfrac{D^3(f)}{3} - \sqrt{\dfrac{\mu}{2q^3}}(t - t_P) & \text{for } e = 1; \\ e\sinh F(e, f) - F(e, f) - \sqrt{\dfrac{\mu}{q^3}}(t - t_P)(\sqrt{e-1})^3 & \text{for } e > 1; \end{cases}$$

The equation $G(q, e, f, t - t_P) = 0$ implicitly defines the true anomaly f as a C^∞ function $f = g(q, e, t - t_P)$ for $q > 0$, $e > 0$ and $t - t_P \in \mathbb{R}$.

Proof If $e < 1$, by differentiating G with respect to f and using (3), we get

$$\frac{\partial G}{\partial f} = (1 - e\cos E)\frac{\partial E}{\partial f} = \frac{\partial E}{\partial f} = \frac{\sqrt{1-e^2}}{1 + e\cos f} \neq 0\,.$$

So, $\partial G/\partial f \neq 0$ and by the implicit function theorem $g \in C^\infty$ for $e < 1$.
If $e > 1$, by differentiating G with respect to D we get

$$\frac{\partial G}{\partial f} = (e\cosh F - 1)\sqrt{\frac{e-1}{e+1}}\left(1 + \tan^2\frac{f}{2}\right)\cosh^2\frac{F}{2} \neq 0\,.$$

By the implicit function theorem $g \in C^\infty$ for $e > 1$.

We have to prove that f in C^∞ for $e = 1$. First we prove that π and $-\pi$ cannot be accumulation points for f. Take $(q_n, (t - t_P)_n, e_n) \to (q, t - t_P, 1)$, such that the corresponding $f_n \to \pi$. Since $r_n = q_n(1 + e_n)/(1 + e_n \cos f_n)$ and the velocity is $\leq \sqrt{\mu(1 + e_n)/q_n}$, the required time to go from the pericenter to the new position is $\geq \sqrt{q_n^3(1 + e_n)/\mu}/(1 + e_n \cos f_n) \to \infty$, that is absurd. For the same reason $-\pi$ is not an accumulation point for f.

Let us take now $(q_n, (t - t_P)_n, e_n) \to (q, t - t_P, 1)$ such that $f_n \to \bar{f}$. Since $\bar{f} \neq \pm\pi$, we have $|1 - e_n|/(1 + e_n)D_n^2 < 1$ for n large enough. Thus, we have that f_n solves

$$\chi_{NP}(e_n, D_n) = \sqrt{\frac{\mu}{2q_n^3}}(t - t_P)_n \, .$$

By taking the limit $e \to 1$ we get that $\bar{D} = \tan \bar{f}/2$ is the solution of Barker's equation. Thus, g is continuous.

By differentiating χ_{NP} with respect to f we get

$$\frac{\partial \chi_{NP}}{\partial f}(e = 1, f = \bar{f}) = \frac{(1 + \bar{D}^2)^2}{2} \neq 0 \, .$$

By the implicit function theorem $g \in C^\infty$ for $e = 1$. □

4 Resolution of Kepler's equation in the near parabolic region

When we are in the near parabolic region, if δ is small enough then $|x| < 1$. Thus, we can apply the theory developed in the previous section. Numerical tests (see Sect. 6) suggest that $\delta = 10^{-2}$ is a sensible choice.

4.1 Computation of t_P

We can compute the pericenter time t_P from f by

$$t_P = t - \sqrt{\frac{2q^3}{\mu}}\chi_{NP}(e, D) \, .$$

4.2 Computation of f

To solve equation $\chi_{NP}(e, D) = M_P$ by using Newton's method we need the derivatives of $\chi_{NP}(e, D)$ with respect to D:

$$\frac{\partial \chi_{NP}(e, D)}{\partial D} = \frac{\sqrt{2}}{\sqrt{1 + e}} + \frac{\sqrt{2}D^2}{\sqrt{1 + e}^3} \sum_{k=0}^{\infty} \left(e - \frac{1}{2k + 3} \right) (2k + 3)x^k \, ,$$

$$\frac{\partial^2 \chi_{NP}(e, D)}{\partial D^2} = \frac{\sqrt{2}D}{\sqrt{1 + e}^3} \sum_{k=0}^{\infty} \left(e - \frac{1}{2k + 3} \right) (2k + 3)(2k + 2)x^k \, .$$

For $e = 1$ we have that

$$\frac{\partial \chi_{NP}(1, D)}{\partial D} = \frac{\sqrt{2}}{\sqrt{1+e}} + \frac{\sqrt{2}}{\sqrt{1+e}^3}\left(e - \frac{1}{3}\right)3D^2 \geq \frac{\sqrt{2}}{\sqrt{1+e}}\,,$$
$$\frac{\partial^2 \chi_{NP}(1, D)}{\partial D^2} = \frac{\sqrt{2}}{(\sqrt{1+e})^3}\left(e - \frac{1}{3}\right)6D \geq 0\,.$$

For $e \geq 1$ the last 2 estimates still hold, as we add non-negative terms only. For $e < 1$ we note that:

$$\chi_{NP}(e, D) = \frac{E - e\sin E}{\sqrt{2}\sqrt{(1-e)^3}}\,,$$
$$\frac{\partial \chi_{NP}(e, D)}{\partial D} = \frac{1 - e\cos E}{\sqrt{2}(1-e^2)}\frac{\sqrt{1+e}}{1-x} > 0\,,$$
$$\frac{\partial^2 \chi_{NP}(e, D)}{\partial D^2} = \frac{3e - 2\sqrt{1-x}}{\sqrt{2}}\frac{(1-e)\sqrt{-x}}{\sqrt{(1-x)^3}}\,.$$

We have that

$$3e - 2\sqrt{1-x} \geq 3e - 2\sqrt{2}$$

which is positive provided that $e > 2\sqrt{2}/3 \simeq 0.94$ (assured if $\delta \leq 10^{-2}$). Furthermore, $\partial_D \chi_{NP}(1, D)$ does not go to 0 as $e \to 1$, since $\chi_{NP}(1, D)$ is C^∞.

As the first derivative is greater than 0 and χ_{NP} convex, we can apply Newton's method:

$$D_{k+1} = D_k - \frac{\chi_{NP}(e, D_k) - M_P}{\partial_D \chi_{NP}(e, D_k)}\,.$$

A starting guess is given by the solution of Barker's equation.

5 Generic resolution

We can use the theory developed in the previous sections to solve Kepler's equation in all eccentricity regimes.

When computing the pericenter time, e and f are known. Thus, we know in which region of Fig. 1 we are and the pericenter time can be computed by the following:

$$t_P = \begin{cases} t - \sqrt{\dfrac{q^3}{\mu(1-e)^3}}(E - e\sin E) & \text{STRONG ELLIPTIC} \\ t - \sqrt{\dfrac{2q^3}{\mu}}\chi_{NP}(e, D) & \text{NEAR PARABOLIC} \\ t - \sqrt{\dfrac{q^3}{\mu(e-1)^3}}(e\sinh F - F) & \text{STRONG HYPERBOLIC} \end{cases}.$$

When trying to compute the true anomaly, the strategy could be the following:

– If $e < 1 - \delta$ we are in the Strong Elliptic case and thus we apply Newton's method to Eq. (4) until convergence.

- If $1-\delta \leq e < 1$ we compute $E_\delta = \arccos((1-\delta)/e)$ and check if the solution belongs to the Strong Elliptic or the Near Parabolic region by comparing $\chi_E(e, E_\delta)$ and M_E. In the Strong Elliptic case we apply Newton's method to Eq. (4) until convergence, otherwise we switch to the formulation of Sect. 4.2. Note that if $D < 0$ the true anomaly is $f = 2\pi + 2\arctan(D)$.
- If $e = 1$ we solve Barker's equation.
- If $1 < e \leq 1+\delta$ we compute $F_\delta = \operatorname{arccosh}((1+\delta)/e)$ and check if the solution belongs to the Strong Hyperbolic or the Near Parabolic region by comparing $\chi_H(e, F_\delta)$ and M_H. In the Strong Hyperbolic case we apply Newton's method to Eq. (7) until convergence, otherwise we switch to the formulation of Sect. 4.2.
- If $e > 1+\delta$ we are in the Strong Hyperbolic case and thus we apply Newton's method to Eq. (7) until convergence.

6 Numerical tests

To test the procedure of Sect. 5 we fixed the units such as $q = 1$ and $\mu = 1$. Then, we took the values of e between 0 and 3 with a step of 10^{-5}. For each value of e we took the values of $t - t_P$ between 0 and 3 with a step of 10^{-2}. When $e < 1$ we selected half orbital period as upper bound for $t - t_P$.

We stopped the iterative procedure when both the following conditions were satisfied:

- the magnitude of the difference in true anomaly between two consecutive iterations was $< 10^{-12}$;
- χ_E (χ_{NP}, or χ_H) changed sign when shifting f_k by 10^{-12}.

We chose $\delta = 10^{-2}$ for the near parabolic switch. Figures 2 and 3 show the number of required iterations: in the elliptic case we never have more than 12 iterations, in the hyperbolic one we always have less than 7 iterations, while in the near parabolic case we mostly have 3 iterations. Moreover, the right panel of Fig. 3 shows that the computation of $S(e, x)$, and thus of χ_{NP}, does not represent an issue, as the number of required terms is never larger than 5. It is worth pointing out that the use of higher order iterative methods and finer starting points would allow better performances in terms of required iterations. However, saving few iterations makes little difference with nowadays CPUs. The most important aspect is that there are no failures, thus proving that the procedure is robust. The selected value of $\delta = 10^{-2}$ prevents the occurrence of numerical issues when $e \simeq 1$. As a comparison, we applied the classical Newton's method without switching to the Near Parabolic formulation. We found 141 failures for $e < 1$ (see left panel of Fig. 4) and 20 for $e > 1$ (see right panel of Fig. 4). As expected all failures arise when $e \sim 1$ thus showing the importance of the formulation presented in this paper.

Figure 5 shows the number of required iterations in the $(\Delta t, e)$ plane. It is interesting to see how for $e < 1$ the number of iterations increases when approaching 1. However, the number of iterations decreases thanks to the near parabolic formulation when $e \sim 1$.

The choice of δ is neither easy nor unique. At the end of Sect. 5 we have seen that to apply Newton's method in the Near Parabolic region for $e < 1$ we need $e > 2\sqrt{2}/3$, that yields $\delta < 1 - 2\sqrt{2}/3 \approx 0.057$. Moreover, we have that δ cannot be too small, otherwise the Near Parabolic region would shrink too much and exclude some singular cases. We repeated the simulation above by using $\delta = 5 \times 10^{-2}$ and $\delta = 10^{-3}$. The procedure turned out to be robust with these choices too as no failures occurred. However, for $\delta = 5 \times 10^{-2}$ we had a slightly larger number of required terms to compute the series S (see left panel of Fig. 6),

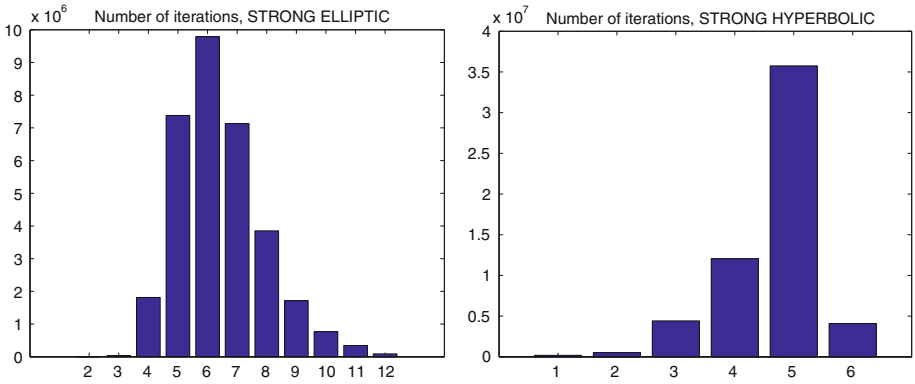

Fig. 2 Number of iterations in the strong elliptic and strong hyperbolic cases

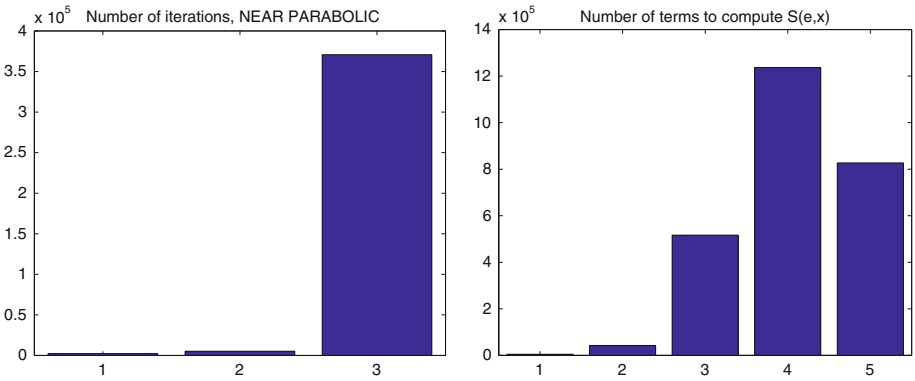

Fig. 3 Number of iterations in the near parabolic case and number of terms required to compute $S(e, x)$

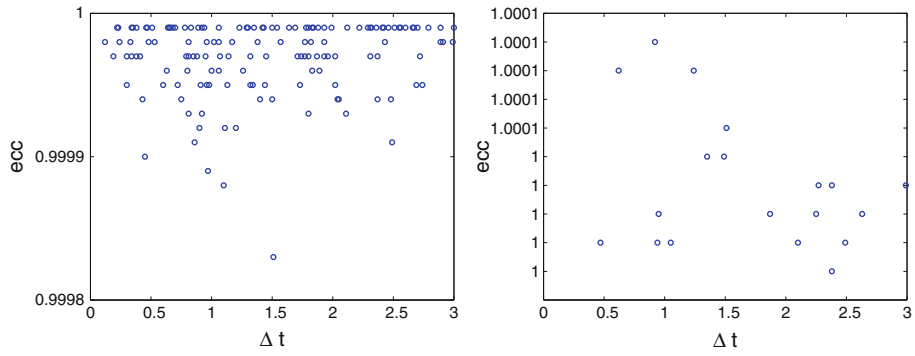

Fig. 4 Failures of the classical Newton's method in the $(\Delta t, e)$ plane

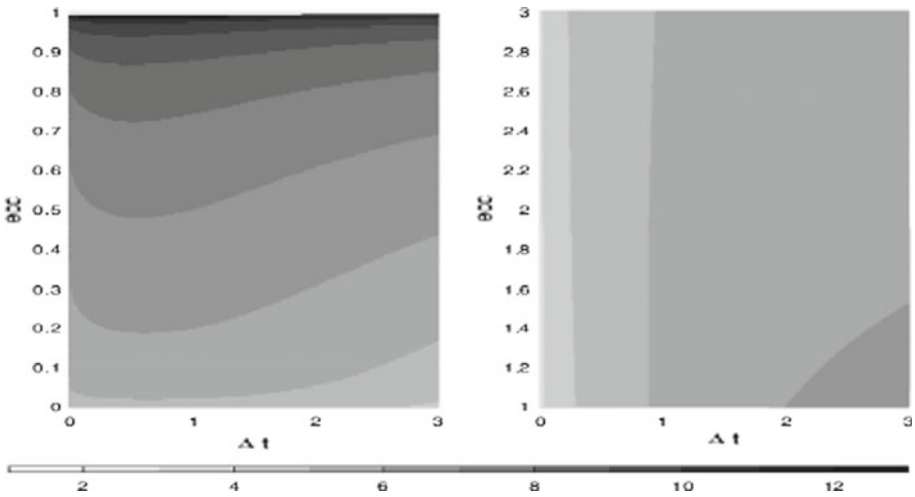

Fig. 5 Number of iterations in the $(\Delta t, e)$ plane. *Left panel* is for $e \leq 1$, *right panel* for $e \geq 1$

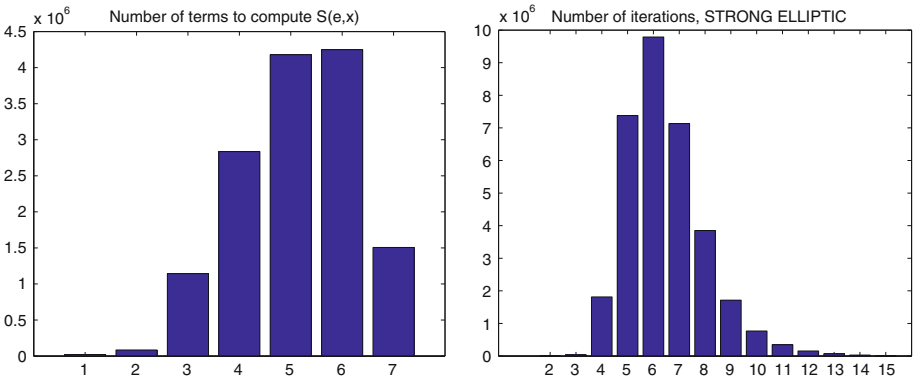

Fig. 6 *Left panel* number of terms required to compute $S(e, x)$ for $\delta = 5 \times 10^{-2}$. *Right panel* number of iterations in the strong elliptic case for $\delta = 10^{-3}$

while for $\delta = 10^{-3}$ the number of required iteration in the Strong Elliptic/Hyperbolic cases slightly increased (see right panel of Fig. 6). As a conclusion, $\delta = 10^{-2}$ seems to strike a good compromise between efficiency and robustness, but other choices are possible.

To prove that Prop. 1 provides a starting point that prevents overflow issues, we performed a test suited for hyperbolic orbits in a wider time range. Namely, we let e range between 1 and 5 with a step of 10^{-2} and $t - t_P$ between 0 and 1000 with a step of 10^{-2}. This grid results in r ranging between q and $2 \times 10^4 q$. Again, we found no failures and the maximum number of iterations was 7, thus showing that also the most extreme cases possibly arising from modern surveys are successfully handled.

7 Conversion between Cartesian coordinates and orbital elements

An application of the method described in Sect. 5 is to perform non-singular conversions between Cartesian coordinates CAR, i.e., position **r** and velocity **v**, and sets of orbital

elements. As a prototype example we describe the conversion to (and from) cometary elements (COM), defined as q, e, I, Ω, ω, t_P. It is convenient to use as intermediate step the COT orbital elements, which are the same as COM apart from t_P that is replaced by f. As a matter of fact, the conversion between CAR and COT is straightforward (Schaub et al. 2009, Chap. 7). So, the difficulty is in the conversion between COM and COT.

Starting from COT elements at time t, we can compute COM elements by using the strategy of Sect. 5. The derivatives of the coordinate change are given by

$$\frac{\partial COM}{\partial COT} = \begin{pmatrix} 1 & 0 & 0 & 0 & 0 & 0 \\ 0 & 1 & 0 & 0 & 0 & 0 \\ 0 & 0 & 1 & 0 & 0 & 0 \\ 0 & 0 & 0 & 1 & 0 & 0 \\ 0 & 0 & 0 & 0 & 1 & 0 \\ \frac{\partial t_P}{\partial q} & \frac{\partial t_P}{\partial e} & 0 & 0 & 0 & \frac{\partial t_P}{\partial f} \end{pmatrix}.$$

Starting from COM elements, we can compute COT at time t elements by solving Kepler's equation as described in Sect. 5. In this case the derivatives are the following:

$$\frac{\partial COT}{\partial COM} = \begin{pmatrix} 1 & 0 & 0 & 0 & 0 & 0 \\ 0 & 1 & 0 & 0 & 0 & 0 \\ 0 & 0 & 1 & 0 & 0 & 0 \\ 0 & 0 & 0 & 1 & 0 & 0 \\ 0 & 0 & 0 & 0 & 1 & 0 \\ -\left(\frac{\partial t_P}{\partial f}\right)^{-1} \frac{\partial t_P}{\partial q} & -\left(\frac{\partial t_P}{\partial f}\right)^{-1} \frac{\partial t_P}{\partial e} & 0 & 0 & 0 & \left(\frac{\partial t_P}{\partial f}\right)^{-1} \end{pmatrix}.$$

From Eq. (2) we immediately get

$$\begin{cases} \dfrac{\partial t_P}{\partial q} = \dfrac{3}{2}\dfrac{t_P - t}{q} \\ \dfrac{\partial t_P}{\partial f} = -\dfrac{1}{(1+e\cos f)^2}\sqrt{\dfrac{q^3(1+e)^3}{\mu}} \end{cases}.$$

On the other hand the derivative of t_P with respect to e depends on the cases:

$$\frac{\partial t_P}{\partial e} = \begin{cases} \sqrt{\dfrac{q^3}{\mu(1-e)^5}}\left[\dfrac{(2+e)\sin E - 3E}{2} + \dfrac{\sin E(1-e\cos E)}{1+e}\right] & \text{STRONG ELLIPTIC} \\ -\sqrt{\dfrac{2q^3}{\mu}}\dfrac{\partial \chi_{NP}}{\partial e} & \text{NEAR PARABOLIC} \\ \sqrt{\dfrac{q^3}{\mu(e-1)^5}}\left[\dfrac{(2+e)\sinh F - 3F}{2} + \dfrac{\sinh F(1-e\cosh F)}{1+e}\right] & \text{STRONG HYPERBOLIC} \end{cases}$$

where

$$\begin{aligned} \frac{\partial \chi_{NP}}{\partial e} = &-\frac{D}{\sqrt{2(1+e)^3}} - \frac{3D^3}{\sqrt{2(1+e)^5}}\sum_{k=0}^{\infty}\left(e - \frac{1}{2k+3}\right)x^k \\ &+\frac{\sqrt{2}D^3}{\sqrt{1+e}^3}\left(1 + \frac{D^2}{(e+1)^2}\sum_{k=0}^{\infty}\left(2ek + 2e + e^2 - 2 + \frac{3}{2k+5}\right)x^k\right). \end{aligned}$$

Note that in the computation of the derivatives the values of both $(t_P - t)$ and E must account for the number of revolutions when $e < 1$.

The conversion to/from other orbital elements can be obtained by composition. As an example, Keplerian orbital elements, i.e., a (semimajor axis), e, I, Ω, ω, and ℓ (mean anomaly), can be easily converted to/from COM and the derivatives are obtained by the chain rule.

8 Comparison with universal variables

Everhart and Pitkin (1983) describe a universal formulation introducing the universal variable ψ that is defined by Sundman's transformation

$$\frac{d\psi}{dt} = \frac{1}{||\mathbf{r}||} .$$

By differentiating (4), (6), and (7) it easy to see that ψ is related to the eccentric anomalies as follows:

$$\psi = \begin{cases} \sqrt{\dfrac{q}{\mu(1-e)}}(E - E_0) & e < 1 \\ \sqrt{\dfrac{q(1+e)}{\mu}}(D - D_0) & e = 1 \\ \sqrt{\dfrac{q}{\mu(e-1)}}(F - F_0) & e > 1 \end{cases} . \tag{9}$$

This universal formulation has the advantage of yielding a unique Kepler's equation regardless the shape of the orbit and is especially suited when the purpose is orbital propagation over short time spans. A numerical method suitable for this formulation is presented in Danby (1987). The limitation of the universal variable formulation is that there is no way to avoid the computation of many large terms in the series defining Stumpff's functions when $t - t_P$ becomes large (Odell and Gooding 1986). It is possible to use half angle formulas, but recursion makes it difficult to control the numerical error.

Another limitation of the universal formulation is that it may be difficult to select a suitable starting point, especially when the time interval is large (with short intervals of time it is possible to use a Taylor's expansion around the initial conditions). A solution could be to use the starting points of the classical formulation and convert them to starting values of ψ by means of (9). Finally, while ψ is the inverse of a velocity, the formulation discussed in this paper has the advantage of using dimensionless variables thus allowing units independent convergence controls.

9 Conclusions

To prevent rounding off issues, we found a starting point to numerically solve Kepler's equation in the hyperbolic case. Then, we described a generalization of Barker's equation for $e \neq 1$ that allows a smooth transition of Kepler's equation around parabolic orbits. By using this generalization we developed an iterative procedure to solve Kepler's equation for all kind of orbits. In particular, the numerical instability arising in the near parabolic region vanishes by directly using the true anomaly as unknown. We proved the robustness and tested

the performances of our method by extensive numerical tests. The theory developed in this paper might be specially suitable to perform orbital element conversions. To this purpose we explicitly computed the partial derivatives involved.

References

Battin, R.H.: An Introduction to the Mathematics and Methods of Astrodynamics. American Institute of Aeronautics and Astronautics, Reston, VA (1987)
Burkardt, T.M., Danby, J.M.A.: The solutions of Kepler's equation. II. Celest. Mech. **31**, 317–328 (1983)
Calvo, M., Elipe, A., Montijano, J.I., Rández, L.: Optimal starters for solving the elliptic Kepler's equation. Celest. Mech. Dyn. Astron. **115** (2013). doi:10.1007/s10569-012-9456-5
Colwell, P.: Solving Kepler's Equation over Three Centuries. Willmann-Bell, Richmond (1993)
Conway, B.A.: An improved algorithm due to Laguerre for the solution of Kepler's equation. Celest. Mech. **39**, 199–211 (1986)
Danby, J.M.A.: The solution of Kepler's equations—Part three. Celest. Mech. **40**, 303–312 (1987)
Danby, J.M.A., Burkardt, T.M.: The solution of Kepler's equation. I. Celest. Mech. **31**, 95–107 (1983)
Davis, J.J., Mortari, D., Bruccoleri, C.: Sequential solution to Kepler's equation. Celest. Mech. Dyn. Astron. **108**, 59–72 (2010)
Everhart, E., Pitkin, E.T.: Universal variables in the two-body problem. Am. J. Phys. **51**, 712–717 (1983)
Feinstein, S.A., McLaughlin, C.A.: Dynamic discretization method for solving Kepler's equation. Celest. Mech. Dyn. Astron **96**, 49–62 (2006)
Fukushima, T.: A fast procedure solving Kepler's equation for elliptic case. Astron. J. **112**, 2858 (1996)
Markley, F.L.: Kepler equation solver. Celest. Mech. Dyn. Astron. **63**, 101–111 (1995)
Mikkola, S.: A cubic approximation for Kepler's equation. Celest. Mech. **40**, 329–334 (1987)
Milani, A., Gronchi, G.F., Farnocchia, D., Knežević, Z., Jedicke, R., Denneau, L., Pierfederici, F.: Topocentric orbit determination: algorithms for the next generation surveys. Icarus **195**, 474–492 (2008)
Mortari, D., Clocchiatti, A.: Solving Kepler's equation using Bézier curves. Celest. Mech. Dyn. Astron. **99**, 45–57 (2007)
Odell, A.W., Gooding, R.H.: Procedures for solving Kepler's equation. Celest. Mech. **38**, 307–334 (1986)
Palacios, M.: Kepler equation and accelerated Newton method. J. Comput. Appl. Math. **138**, 335–346 (2002)
Schaub, H., Junkins, J.L., Schetz, J.A.: Analytical Mechanics of Space Systems, 2nd edn. American Institute of Aeronautics and Astronautics, Reston, VA (2009)